JOURNAL OF AIRCRAFT
Vol. 29, No. 5, Sept.–Oct. 1992

Flight Measurements of Downwash on the Ball-Bartoe Jetwing Powered Lift Aircraft

U. P. Solies*
University of Tennessee Space Institute, Tullahoma, Tennessee 37388

Flight tests were conducted with the "Ball-Bartoe Jetwing" powered lift technology demonstration aircraft to visualize flow angles on the fuselage surface and at selected points in the flowfield near the horizontal tail. Simple data acquisition techniques were used. The results were used to calculate the downwash near the horizontal tail and its variation with airspeed, jet deflection angle, and blowing coefficient over a range of level flight conditions. Further research is needed to broaden the database and substantiate these findings.

Nomenclature

C_J = blowing coefficient
C_L = aircraft lift coefficient
$C_{L_{\alpha T}}$ = horizontal tail lift curve slope
$C_{L_{\delta T}}$ = elevator effectiveness
$\bar{c}$ = mean aerodynamic chord
F = thrust
h = altitude
i = incidence angle of wing or tail; positive for leading edge up
N = engine rotor speed
q = freestream dynamic pressure
S = wing reference area
V = volume
v = airspeed or flow velocity
W = weight of aircraft
α = geometric angle of attack of the wing
ΔP = duct dynamic pressure
δ = atmospheric pressure ratio or deflection angle of flap
ε = downwash angle; downwash positive
$\bar{\varepsilon}$ = local upwash angle at the rake caused by the lift generation of the horizontal tail; upwash positive
θ = atmospheric temperature ratio
μ = tuft angle, i.e., flow angle relative to the stabilizer chord line

Subscripts

c = corrected
e = elevator
F = flaps
f = fuel
G = gross
i = indicated
m = measured
p = pressure
rem = remaining
T = tail
t = test
W = wing
∞ = freestream
1 = primary

Presented as Paper 90-1284 at the AIAA/SFTE/DGLR/SETP 5th Biannual Flight Test Conference, Ontario, CA, May 21–24, 1990; received Jan. 30, 1991; revision received Oct. 15, 1991; accepted for publication Oct. 29, 1991.

*Assistant Professor, Departments of Aviation Systems and Aerospace Engineering, MS-01. Member AIAA.

I. Introduction

THE underlying principle of "powered-lift" technology is the basic jet-flap as first proposed by Schubauer[1] and Hagedorn and Ruden.[2] This technology's aerodynamic advantage is the induced circulation lift (Fig. 1) offering much higher lift coefficients than mechanical high-lift devices. Powered lift aircraft can therefore be designed to combine short takeoff and landing (STOL) operation, steep approaches and departures, and high maneuverability, with small and light wings for high speed and efficient cruise.

One of the problem areas encountered with jet-flapped wings is the high downwash in the flowfield behind it and the corresponding impact on stability and control of powered-lift vehicles. While several theoretical methods have been developed,[3–5] few experimental data of downwash measurements in the presence of a jet sheet are available.[6–8] The aim of this research effort was the establishment of a small database of measured flow angles to serve as reference for theoretical investigations.

II. Description of Test Vehicle

In 1976, the Ball Aircraft Company of Colorado developed an experimental jet aircraft as a technology demonstration vehicle for powered lift.[9–11] The Ball-Bartoe Jetwing represents a low-cost, single-engine, small flight-test bed with a low aspect ratio and uniform blowing over major portions of the wing. This is the first and only single-engine upper surface blown (USB) aircraft built to date (Fig. 2). The Jetwing achieves upper surface blowing from a single Pratt and Whitney JT15D1 turbofan engine by ducting all air through the front portion of the wing and ejecting it over the upper wing surface through

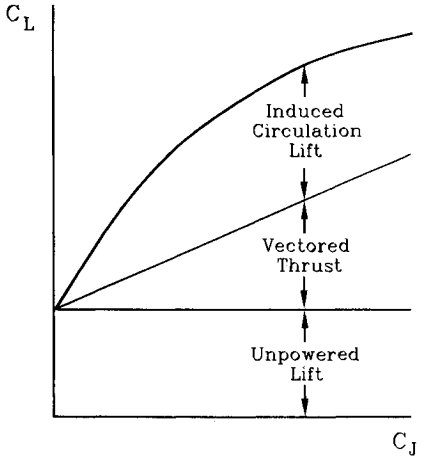

Fig. 1 Lift components of a jet-flapped wing.

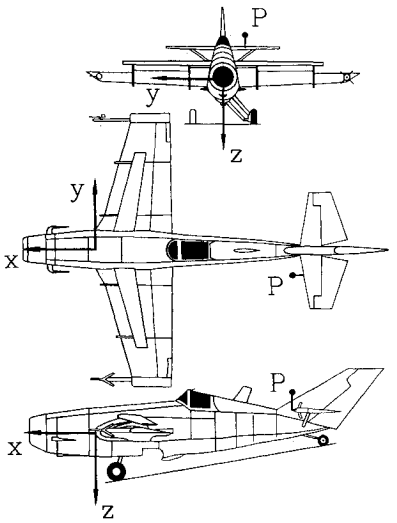

Fig. 2 Ball-Bartoe Jetwing upper surface blown experimental aircraft and location of reference point P ($x, y, z = -5.0, -0.6, -0.972$ m).

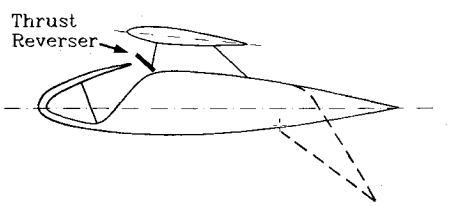

Fig. 3 Two-dimensional view of Jetwing concept.

a slot nozzle. The nozzle is located at 33% of the wing chord and extends along 70% of the wing span, approximately. Bypass air is ducted to the outboard portion of the wing while the core exhaust is ducted to the inboard portion. A removable small wing surface is located above the slot nozzle and acts as an ejector or thrust augmentor. A Coanda-type, single-element flap is located at the trailing edge of the wing along the blown portion of the wing span. Figure 3 shows a two-dimensional sketch of the Jetwing concept. The top of the bypass air nozzle can be rotated to act as a thrust reverser.

The Jetwing research aircraft and its conceptual patents are now owned by The University of Tennessee. It has undergone extensive full scale wind-tunnel tests at NASA Ames Research Center and was flown approximately 70 h by Ball-Bartoe prior to being donated to The University of Tennessee. At UTSI the aircraft was subjected to 97 h of flight testing under contract to the Naval Air Systems Command. The aircraft's performance and handling characteristics were evaluated with and without the upper wing.[12,13]

These test programs and analytical studies[7,13] confirmed the Jetwing concept's capabilities for STOL operation, low speeds, steep approaches, tight maneuvers, and low noise levels. The full potential of the concept could not be demonstrated in flight test due to longitudinal instability of the research aircraft and the loss of longitudinal control at low airspeeds. These characteristics are the results of poor design of the test vehicle rather than an inherent flaw in the concept.

III. Flight Tests

Since the funds for this research project were very limited, the cost for all equipment had to be kept to a minimum. Data acquisition had to rely on existing equipment and relatively simple methods. The chosen procedure represents a compromise between low cost and required accuracy.

Flow visualization was achieved through woolen tufts that were taped at selected surfaces on the test vehicle and a rake that was mounted to the leading-edge of the horizontal tail. The tufts on the vehicle surface were photographed from a camera in a chase aircraft in close formation flight, and the

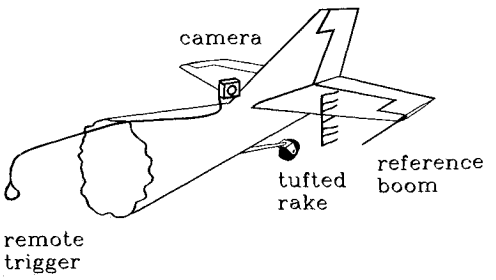

Fig. 4 Experimental setup for downwash angle measurements.

rake was photographed by a camera that was mounted on the test vehicle as shown in Fig. 4. This camera had an automatic film advance capability and a remote trigger that was operated by the pilot of the test aircraft. In addition to the photographic recording of flow angles, the pilot read data from panel instruments and transmitted them by means of a radio to a ground station, where they were hand-recorded.

To facilitate the correlation between the photographic pictures and the hand-recorded data from panel instruments, a digital clock was installed in the view field of the tail-mounted camera. Also, in order to have a reference line for the flow angles indicated by the woolen tufts on the rake, a small boom was mounted on the tip of the stabilizer, marking the extension of the chord centerline of the horizontal tail.

Flight tests were conducted for a matrix of different airspeeds and flap settings. For each data point, the test aircraft was stabilized in level flight and the pilot triggered the tail-mounted camera. At the same time the following data were recorded 1) δ_e—elevator deflection, 2) i_T—tail incidence, 3) α—angle-of-attack, 4) v_i—indicated airspeed, 5) h_{pi}—indicated pressure altitude, 6) OAT—outside air temperature, 7) N_1—engine primary rotor speed, 8) ΔP_{hot}—hot duct dynamic pressure, 9) ΔP_{cold}—cold duct dynamic pressure, and 10) V_{frem}—fuel remaining.

Items 4–7 were displayed on standard instruments; the other data were also readily available from special instrumentation that had been installed in the aircraft for previously conducted flight test programs. A detailed description of the instrumentation set up in the test vehicle can be found in Ref. 12.

IV. Data Evaluation

During the preliminary testing of the tail-mounted camera equipment, some photographs were made with a rectangular grid held in the field of vision. This allowed the checking of pictures for distortions that may have been introduced by the wide-angle lens and angularities in the camera mount. The angular distortions proved to be negligible; therefore the flow angles indicated on the photographs by the tufts were true angles and could easily be measured with a protractor.

Most tufts on the rake showed flutter at some angle and airspeed. Those tufts were not considered for the flow angle determinations. Later in the program, all tufts were shortened from 6 to 4 in.; that reduced the flutter tendency substantially.

Due to the closeness to the leading-edge of the stabilizer, the flow angles indicated by the tufted rake were influenced by the horizontal tail. The top end of the rake was least influenced by the tail and was chosen for quantitative data representation of downwash angles (point P in Fig. 2). Since the main objective of this research was the measured air flow angle change due to the lifting wing and jet sheet, ε_m, the additional changes induced by the horizontal tail were estimated by means of a lifting-line computer program and subtracted from the data. This resulted in downwash angles ε_{mc}, corrected for the influence of the horizontal tail.

The data reduction sequence and the flow angle correction method are outlined as follows. All panel data were corrected for instrument errors; airspeed and altimeter readings were also corrected for position errors. From the calibrated flight test data the following quantities were calculated[11]: true air-

speed, air density at test altitude, aircraft weight at test time (the center of gravity position was typically at $0.35\bar{c}$ and changed very little during test flights), and lift coefficients for aircraft and wing.

The aircraft lift coefficient is

$$C_L = (W_t/qS) \tag{1}$$

Assuming $q_T = q$, the wing-lift coefficient becomes

$$C_{L_W} = C_L - (S_T/S)C_{L_T} \tag{2}$$

where the tail-lift coefficient could be determined as

$$C_{L_T} = C_{L_{\alpha T}}\alpha_T + C_{L_{\delta T}}\delta_e \tag{3}$$

with

$$\alpha_T = \mu_c \tag{4}$$

the measured flow angle at the tail, corrected for the lift-induced flow disturbance by the tail itself, as shown below. The tail-lift curve slope $C_{L_{\alpha T}}$ and the elevator effectiveness $C_{L_{\delta T}}$ could be obtained from diagrams in Ref. 14.

The blowing coefficient is

$$C_J = (F_G/qS) \tag{5}$$

where the gross thrust F_G is a function of δ, θ,[15,16] and the engine rotor speed N_1, and could be determined from a calibration diagram that was established in Ref. 17. The duct pressure data were used to verify the gross thrust.[18]

The angle of attack is

$$\alpha = f(C_L, C_J) \tag{6}$$

This angle between the freestream direction and the wing chord line is difficult to measure in flight. The Jetwing angle-of-attack sensors, mounted on the side of the forward fuselage and on a wingtip boom, are both subject to angular distortions of the flowfield about the airplane and its lifting surfaces. Therefore, the angle-of-attack was determined by entering the C_L and C_J values into the proper wind-tunnel data diagrams.[7]

Since the wing has no incidence, the wing angle-of-attack is identical to the angle-of-attack of the fuselage axis or waterline. With the tail incidence i_T from flight test data and the tuft angle μ measured from the photograph, the measured downwash angle could be determined according to Figs. 5 and 6:

$$\varepsilon_m = \alpha + i_T - \mu \tag{7}$$

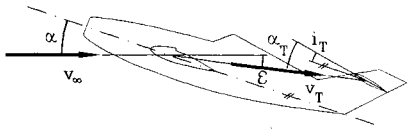

Fig. 5 Flow angles at the horizontal tail.

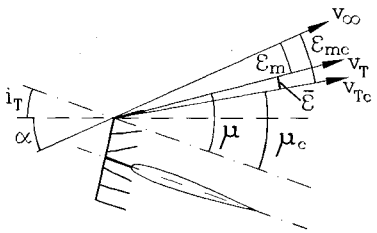

Fig. 6 Flow angles at the tufted rake.

To correct the measured flow angles at the rake for distortions from the horizontal tail, the following procedure was used:

1) With the horizontal tail geometry, and elevator deflection from flight test data, the computer program set up a vortex-lattice system that was allowed to compute the flowfield around it.

2) With air density and velocity data from the flight tests, and the measured tuft angle μ from photographs as a first approximation for the tail angle-of-attack α_T, the program computed the flow angle distortion $\bar{\varepsilon}$ at the top of the rake. This angle represented the upwash caused by the lifting tail at the top tuft location.

3) A new tail angle-of-attack was computed as

$$\alpha_T = \mu - \bar{\varepsilon} \tag{8}$$

and was used as an input value for a new $\bar{\varepsilon}$ computation. The procedure was repeated and converged rapidly toward a final value of $\bar{\varepsilon}$.

4) The corrected downwash angle ε_{mc} for each data point was determined as

$$\varepsilon_{mc} = \varepsilon_m + \bar{\varepsilon} \tag{9}$$

V. Results and Discussion

The measured downwash angles ε_m at the top of the tail mounted rake, as well as the downwash angles ε_{mc}, that are corrected for the influence of the horizontal tail, are shown as a function of jet-flap deflection, airspeed, wing-lift coefficient, blowing coefficient, and wing or fuselage angle-of attack in Figs. 7–10.

All diagrams imply steady, unaccelerated flight conditions; the flights with 45 deg flap deflections resulted in descents (approximately 200 ft/min), while all others were level flights.

In Fig. 8 the wing-lift coefficient was chosen over the aircraft-lift coefficient, because for each airspeed, the shape of the trailing jet sheet and the flowfield around it are mainly influenced by the wing angle of the attack, flap deflection, and the amount of blowing. These parameters relate to the wing-lift coefficient, whereas the aircraft-lift coefficient varies with the tail-load, which is required to trim the aircraft and varies with airspeed and center of gravity position. The wing-lift coefficient is therefore a more meaningful parameter for flow angle presentation.

The figures reveal the following observations:

First, the measured downwash angles are quite substantial, varying between 5.6 deg for a flaps-up, high-speed condition to 25.3 deg for a flaps-down, low-speed condition (immediately after transmitting the data for this point, the pilot reported a tail stall with subsequent pitch-down of the vehicle) (Fig. 7). As expected, the downwash increases with increasing angle of attack (Fig. 10) and blowing coefficient (Fig. 9), which corresponds to increasing wing-lift coefficient (Fig. 8), and reducing airspeed (Fig. 7).

The downwash also increases generally with flap deflection, except for the zero flap condition, where it becomes exceedingly high at low airspeeds and corresponding high values of C_{L_W}, C_J, and α.

The largest measured downwash angle of $\varepsilon_m = 25.3$ deg occurred at the 60 kt, 45 deg flaps condition. For this, the tail-induced downwash was estimated theoretically to be $|\bar{\varepsilon}| = 5.7$ deg, leaving a wing-induced downwash angle of $\varepsilon_{mc} = 19.6$ deg. This is close to the tail-stall condition of the present vehicle configuration.

Figure 8b is of particular interest, since in this diagram of corrected downwash angles vs wing-lift coefficient, the curves for the higher flap settings practically collapse to a single curve. This is in agreement with the theoretical finding,[3–5] that the downwash at a sufficiently large distance from the lifting wing is predominately a function of circulation and therefore, lift coefficient, regardless of whether the circulation

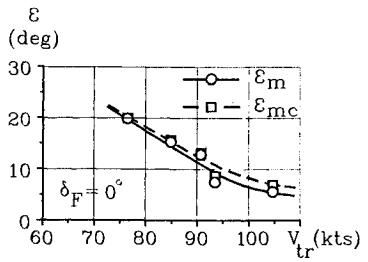

a) 0 deg flap setting

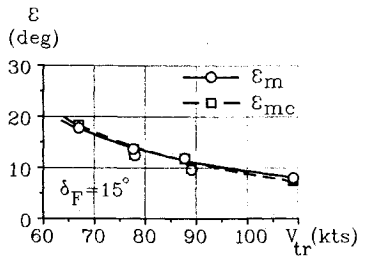

b) 15 deg flap setting

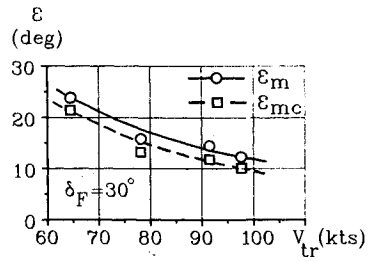

c) 30 deg flap setting

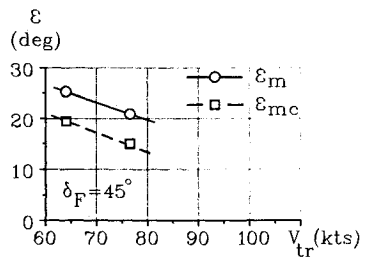

d) 45 deg flap setting

Fig. 7 Measured and corrected downwash angles vs true airspeed.

is generated by angle-of-attack, flap deflection, powered lift, or a combination of these.

The somewhat odd behavior of the downwash at $\delta_F = 0$ can be explained by two conflicting effects which influence the flow angles at the tail:

1) Flap deflection increases the wing circulation and, therefore, the downwash in the flowfield behind it.[4]

2) Flap deflection increases the distance between the tail and the trailing jet sheet. This reduces the downwash at the tail, since downwash increases with proximity to the trailing vortex sheet.[5]

Obviously the first effect dominates the downwash behavior for the higher flap deflections, while the second one dominates it at flight conditions with zero flap settings. In addition, the downwash at a specified point is sensitive to the particular geometry of the jet sheet and trailing vortices.[7]

Second, the diagrams reveal some information about the flow distortion by the tail itself. The angle $\bar{\varepsilon}$ is directly related to the tail load L_T, that balances the pitching moments of the aircraft for each flight condition.

A tail download ($L_T < 0$) causes an additional downwash ($\bar{\varepsilon} < 0$) at the rake, that results in a required reduction of

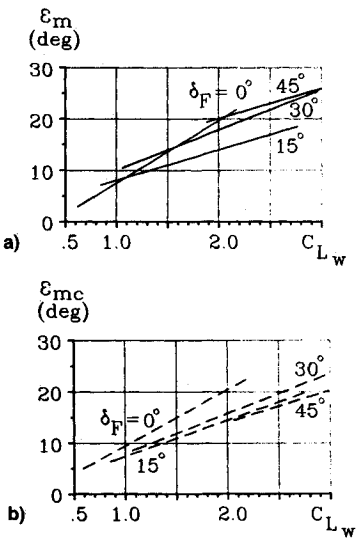

Fig. 8 a) Measured and b) corrected downwash angle vs wing-lift coefficient at various flap settings.

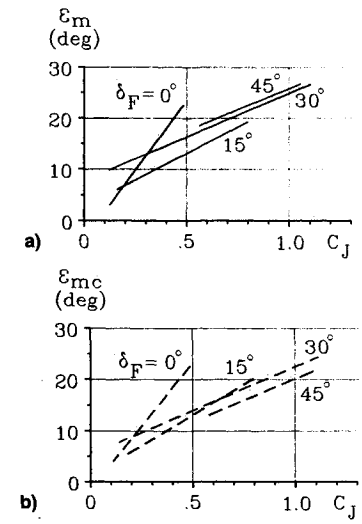

Fig. 9 a) Measured and b) corrected downwash angle vs blowing coefficient at various flap settings.

the measured wing downwash angle ε_m, so that $\varepsilon_{mc} < \varepsilon_m$. On the other hand, an upload on the tail leads to $\varepsilon_{mc} > \varepsilon_m$.

The maximum tail-induced flow distortion $\bar{\varepsilon} = -5.7$ deg occurs for the largest flap deflection, $\delta_F = 45$ deg. This was expected, since for this condition the wing generates a strong nose-down pitching moment that has to be balanced by a significant tail download. For $\delta_F = 30°$, the distortion averages $\bar{\varepsilon} = -2.5$ deg, and practically vanishes for $\delta_F = 15$ deg. For $\delta_F = 0$ deg the distortion becomes positive and increases with airspeed, indicating an upload on the tail, and a positive pitching moment of the wing-fuselage combination. This is contrary to most conventional aircraft with negative pitching moments and increasing tail downloads at higher airspeeds, but it agrees with the Jetwing's airfoil characteristics (modified NACA 23020/15), the aft c.g. position, and the fact that the thrust line is below the c.g. for this flap position.

Third, the slopes of the ε vs α curves give some indication about the change of downwash with wing angle-of-attack; however, these $d\varepsilon/d\alpha$ values imply thrust and airspeed changes and differ therefore from the pitch stability parameter $\partial\varepsilon/\partial\alpha$:

$$\frac{d\varepsilon}{d\alpha} = \frac{\partial\varepsilon}{\partial\alpha} + \frac{\partial\varepsilon}{\partial C_J}\frac{\partial C_J}{\partial\alpha} + \frac{\partial\varepsilon}{\partial v}\frac{\partial v}{\partial\alpha} + \ldots \qquad (10)$$

The partial derivative $\partial\varepsilon/\partial\alpha$ implies α-disturbances at constant airspeed and thrust and must be $\partial\varepsilon/\partial\alpha < 1$, for the tail to be

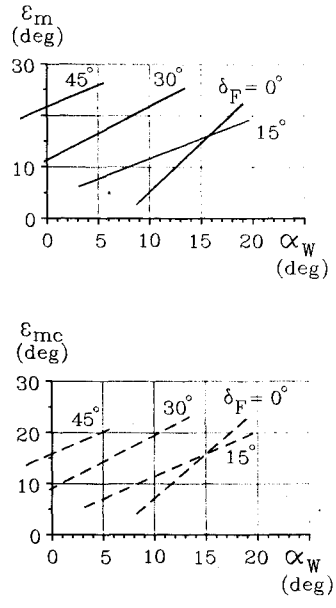

Fig. 10 a) Measured and b) corrected downwash angle vs wing angle-of-attack at various flap settings.

stabilizing.[14] The $d\varepsilon/d\alpha$ term, therefore, relates to trim changes in steady-level flight conditions rather than directly to pitch stability. For the Jetwing, the slope is maximum, $d\varepsilon/d\alpha = 2$, for $\delta_F = 0$ deg. The pilot also reports the poorest longitudinal stability of the aircraft at this configuration.

VI. Conclusions and Recommendations

The downwash angle at the selected point near the horizontal tail of the Ball-Bartoe Jetwing generally increases with wing angle-of-attack and blowing coefficient. Lowering the USB flap also increases the downwash, except that for zero deflection and high angles-of-attack the downwash exceeds that of higher flap settings. This can be contributed to the closeness of the trailing jet sheet to the downwash reference point for this condition. For most cases, the downwash can be expressed as a function of wing-lift coefficient only.

More data points are needed to isolate the influence of scatter. Additional measurements at conditions other than level flight are recommended to allow the extraction of pitch stability parameters, e.g., $\partial\varepsilon/\partial\alpha$. Also, different locations along the tail span as well as near the top of the vertical tail should be investigated, to point toward the benefits of a T-tail and other tail modifications.

References

[1]Schubauer, G. B., "Jet Propulsion with Special References to Thrust Augmentations," NACA TN 442, 1933.

[2]Hagedorn, H., and Ruden, P., "Windkanal Untersuchungen as einem Junkers Doppelfluegel mit Ausblaseschlitz am Knick des Hauptfluegels," *Technischer Bericht des Institutes fuer Aeromechanik und Flugtechnik der Technischen Hochschule Hannover*, Lilienthal Gesellschaft, Bericht A64, 1938.

[3]Spence, D. A., "The Lift on an Aerofoil with a Jet-Augmented Flap," *The Aeronautical Quarterly*, Vol. 9, Pt. 3, Aug. 1958, pp. 287–299.

[4]Jacobs, W. F., "Theory of the Jet-Augmented Flap in Three Dimensions," Lockheed-Co., Rept. LG 73 E R0023, Marietta, GA, Dec. 1972.

[5]Ross, A. J., "The Theoretical Evaluation of the Downwash Behind Jet-Flapped Wings," A.R.C. R&M No. 3119, London, 1961.

[6]Eppel, J. C., Riddle, D. W., and Stevens, V. C., "Flight Measured Downwash of the QSRA," *Fourth Flight Test Conference*, AIAA Paper 88-2141, San Diego, CA, May 1988.

[7]Solies, U. P., "A Study of the Flow Field About an Upper Surface Blown Wing and its Effects on Longitudinal Static Stability of a Small Jet Airplane," Ph.D. Dissertation, Univ. of Tennessee Space Inst., Tullahoma, TN, 1985.

[8]Solies, U. P., "In Flight Flow Angle Measurements on the Ball-Bartoe Jetwing Powered Lift Aircraft," *Fifth Flight Test Conference*, AIAA Paper 90-1284, Ontario, CA, May 1990.

[9]"Jetwing from Colorado," *Air International*, Vol. 14, No. 2, 1978. pp. 69–71.

[10]Anon., "Jetwing, a Very Quiet Machine," *Professional Pilot*, Vol. 12, No. 4, 1978, pp. 16–19.

[11]Fink, D. E., "Propulsive Lift Concepts Flight Tested," *Aviation Week and Space Technology*, Vol. 107, No. 12, 1977.

[12]Kimberlin, R. D., "A Flight Test Evaluation of the Ball-Bartoe Jetwing Propulsive Lift Concept," Univ. of Tennessee Space Inst., UTSI Rept. 81-1, Tullahoma, TN, July 1981.

[13]Kimberlin, R. D., Solies, U. P., and Sinha, A. K., "A Flight Test Evaluation and Analytical Study of the Ball-Bartoe Jetwing Propulsive Lift Concept without Ejector," Univ. of Tennessee Space Inst., UTSI Rept. 82/17, Tullahoma, TN, Oct. 1, 1982.

[14]Etkin, B., *Dynamics of Flight—Stability and Control*, 2nd Ed., Wiley, New York, 1982.

[15]Herrington, R. M., Schoemacher, P. E., Bartlett, E. P., Dunlap, E. W., "*USAF Flight Test Engineers Handbook*," Air Force Flight Test Center, AF-TR No. 6273, Edwards AFB, CA, 1961, Rev. 1966.

[16]Anon., "United States Standard Atmosphere," NACA TR 1235, 1962.

[17]Trimbach, J. M., "The V-γ Performance Method as Applied to the Ball-Bartoe Jetwing STOL Aircraft," M.S. Thesis, Univ. of Tennessee Space Inst., Tullahoma, TN, June 1981.

[18]Rooke, K. A., "An Evaluation of Nozzle Pressure Ratio as a Means of Determining In-Flight Gross Thrust of the Ball-Bartoe Jetwing with the Pratt and Whitney JT 15 D-1 Turbofan Engine Installed," M.S. Thesis, Univ. of Tennessee Space Inst., Tullahoma, TN, Aug. 1980.